

increase in the vertex inversion barrier height over that for PH_3 would have been expected due to the presence of the electro-negative ligands in **1**.² The significant decrease in the barrier height for **1c** argues strongly that we are indeed observing edge inversion. The low value for ΔS^\ddagger is consistent with a unimolecular process as would be expected for simple inversion. Thus, it is unlikely that a bimolecular process is leading to the low value for the inversion barrier observed for **1c**.

In order to gain insight into the experimental results, we have performed high-level ab initio molecular orbital calculations on the edge inversion process. The geometries for the pyramidal **1a** (C_3 symmetry) and planar T-shaped **2a** (C_{2v} symmetry) forms were gradient optimized^{9,10} at the self-consistent field (SCF) level with a double- ζ basis set¹¹ augmented by sets of d polarization functions on P, O, and N.

The most important structural features are the bonding parameters at phosphorus. The P-O bond distances are 1.634 Å, and the P-N bond distance is 1.749 Å for pyramidal **1a**. The OPN bond angles are 93.6°, consistent with normal bond angles at tricoordinate phosphorus,⁸ while the O-P-O bond angle is opened up to 106.0°. The lengths of the bonds to phosphorus reverse in planar **2a**. The P-O bond distances have lengthened to 1.718 Å while the P-N bond distance has decreased to 1.660 Å, consistent with our previous calculations on PF_3 .² As would be expected for a T-shaped planar structure, the OPO group is approximately linear with an OPO bond angle of 172.7° (the OPN bond angles are 86.4°). At this level of calculation, the inversion barrier is 43.0 kcal/mol.

From the optimized geometries for **1a** and **2a**, the energies were recalculated¹² with a slightly larger basis set¹³ both at the SCF level and including correlation effects at the MP2-level.¹⁴ The energy difference at the SCF level is 43.5 kcal/mol, in excellent agreement with the SCF value given above. Inclusion of the MP-2 correction lowers the inversion barrier to 28.1 kcal/mol. The large correlation correction of 15.4 kcal/mol is typical of edge inversion processes¹⁵ while vertex inversion usually involves only a small correlation correction;¹⁶ for example, the correlation correction to the vertex inversion barrier in PH_3 is 2 kcal/mol.⁸

The calculated inversion barrier for **1a** is 4.7 kcal/mol higher than the measured inversion barrier for **1c**. This difference may be due to a number of factors. There is considerable difference between adamantyl and hydrogen as a substituent especially in terms of steric bulk. The steric bulk of the adamantyl group could cause the five-membered ring to adopt a higher energy configuration in the pyramidal form thus lowering the inversion barrier.

Another reason for the difference is that our calculated value is an upper limit at this level of calculation. The force fields for **1a** and **2a** were determined analytically. Structure **1a** has no imaginary frequencies and is thus a minimum on the potential energy surface. If planar **2a** were a transition state, it would have a single imaginary frequency. For the structure with all of the heavy atoms in a plane, three imaginary frequencies are found

and thus our structure is slightly higher in energy than the actual transition state. The largest imaginary frequency (188i cm^{-1}) is the measure of curvature for the inversion mode. The two smaller imaginary frequencies (84i and 30i cm^{-1}) are very low (the sum of the latter two frequencies is 0.33 kcal/mol) and correspond to torsions about the C-C bonds. Since the CH_2 groups are in an eclipsed conformation, this leads to an increase in the energy. Furthermore, the MP2 correction may not be recovering all of the correlation energy difference between the planar and pyramidal forms. All of these arguments are consistent with the observed difference between theory and experiment.

Acknowledgment is made to Dr. T. Fukunaga for helpful discussions throughout the course of this work and to M. Kline for excellent technical assistance in the synthesis of **3** and **1c**. F. Davidson provided the ³¹P, ¹⁵N, and ¹⁷O spectra reported herein.

Synthetic Methodology for Polyoxocyclopentadienyltitanium Complexes: Synthesis and Structure of $\text{L}_6\text{Ti}_6\text{O}_{8-n}\text{Cl}_n$ ($\text{L} = \eta^5\text{-C}_5\text{H}_5$, $\eta^5\text{-C}_5\text{H}_4\text{CH}_3$; $n = 4, 2, 0$)

Alan Roth,[†] Carlo Floriani,^{**} Angiola Chiesi-Villa,[‡] and Carlo Guastini[‡]

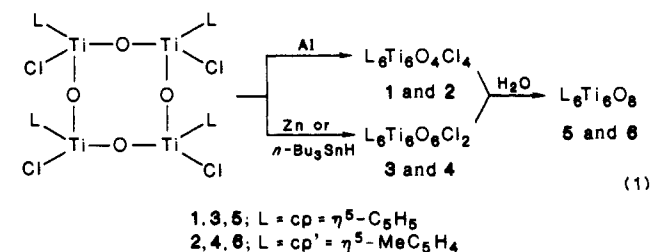
Chemistry Department, Columbia University
New York, New York 10027

Istituto di Strutturistica Chimica, Centro di
Studio per la Strutturistica Diffratometrica del CNR
Università di Parma, 43100 Parma, Italy

Received May 27, 1986

Polyoxo- and polyoxochloro organometallic aggregates which do not contain weak metal-metal bonds have several attractive properties. Some of them have been masterly brought into focus by a review from Klemperer and Day on polyoxoanions.¹ In particular, the aggregates may display interesting magnetic properties, cooperative chemical behavior, and geometrical proximity of reactive sites. Synthetically, we became interested in electron-rich and functionalizable aggregates which are not accessible by the common methodologies,¹ including the controlled oxidation of metal cyclopentadienyl derivatives recently devised by Bottomley.² We report a synthetic procedure, based on the use of reducing agents, for transforming cyclopentadienyloxochloro complexes of titanium(IV) into the building block of aggregates having the formula $[\text{cp}_6\text{Ti}_6\text{O}_{8-n}\text{Cl}_n]$ and $[\text{cp}'_6\text{Ti}_6\text{O}_{8-n}\text{Cl}_n]$ ($\text{cp} = \eta^5\text{-C}_5\text{H}_5$ and $\text{cp}' = \eta^5\text{-MeC}_5\text{H}_4$; $n = 4, 2, 0$). One member of the two series, $\text{cp}_6\text{Ti}_6\text{O}_8$, has already been reported.³

We carried out the reduction of $[\text{cpTiCl}(\mu\text{-O})]_4$,⁴ $[\text{cp}'\text{TiCl}(\mu\text{-O})]_4$,⁵ and $[\text{cpTiCl}_2]_2(\mu\text{-O})$ as shown in eq 1 and following the



(9) (a) Komornicki, A.; Ishida, K.; Morokuma, K.; Ditchfield, R.; Conrad, M. *Chem. Phys. Lett.* **1977**, *45*, 595. McIver, J. A.; Komornicki, A. Jr. *Ibid.* **1971**, *10*, 303. (b) Pulay, P. In *Applications of Electronic Structure Theory*; Schaefer, H. F., Ed.; Plenum: New York, 1977; p 153.

(10) (a) Dupuis, M.; Rys, J.; King, H. F. *J. Chem. Phys.* **1976**, *65*, 111. (b) King, H. F.; Dupuis, M.; Rys, J. *National Resource for Computer Chemistry Software Catalog*, Vol 1, Program QHO2 (HONDO) 1980.

(11) Dunning, T. H., Jr.; Hay, P. J. In *Methods of Electronic Structure Theory*, Schaefer, H. F., III, Ed.; Plenum Press: New York, 1977; Chapter 1. $3d \zeta(p) = 0.50$. The basis set is (11s7p1d/9s5p1d/9s5p1d/9s5p/4s)/[6s4p1d/3s2p1d/3s2p1d/3s2p/2s] in the order P, O, N, C, H.

(12) GRADSCF is an ab initio gradient system designed and written by A. Komornicki at Polyatomic Research and supported on grants through NASA-Ames Research Center.

(13) The basis set is (13s9p1d/9s5p1d/9s5p1d/9s5p/4s)/[6s4p1d/4s2p1d/4s2p1d/2s]. The s and p orbital coefficients and exponents for C, N, O, and H are from: Dunning, T. H., Jr. *J. Chem. Phys.* **1970**, *53*, 2823. Those for P are from: McLean, A. D.; Chandler, G. S. *J. Chem. Phys.* **1980**, *72*, 5639. The exponents for the polarization functions are those given in ref 12.

(14) (a) Möller, C.; Plesset, M. S. *Phys. Rev.* **1934**, *46*, 618. (b) Pople, J. A.; Binkley, J. S.; Seeger, R. *Int. J. Quantum Chem. Symp.* **1976**, *10*, 1.

(15) Dixon, D. A.; Arduengo, A. J., III, unpublished results.

(16) Freed, K. F. *Chem. Phys. Lett.* **1968**, *2*, 255.

* Present address: I.C.M.A., Université de Lausanne, CH-1005 Lausanne, Switzerland.

[†] Columbia University.

[‡] Università di Parma.

(1) Day, V. W.; Klemperer, W. G. *Science (Washington, D.C.)* **1985**, *228*, 533-541 and references therein.

(2) Bottomley, F.; White, P. S. *J. Chem. Soc., Chem. Commun.* **1981**, 28-29. Bottomley, F.; Paez, D. E.; Sutin, L.; White, P. S. *Ibid.* **1985**, 597-598. Bottomley, F.; Paez, D. E.; White, P. S. *J. Am. Chem. Soc.* **1985**, *107*, 7226-7227. (b) *Ibid.* **1982**, *104*, 5651-5657. Bottomley, F.; Darkwa, J.; White, P. S. *J. Chem. Soc., Dalton Trans.* **1985**, 1435-1442.

(3) Huffman, J. C.; Stone, J. G.; Krussel, W. C.; Caulton, K. G. *J. Am. Chem. Soc.* **1977**, *99*, 5829-5831.

(4) Gorsich, R. D. *J. Am. Chem. Soc.* **1960**, *82*, 4211-4214.

detailed procedures reported for **2** and **3**.⁶ The chlorooxo compounds **1–4** are very reactive toward H₂O and convert easily into the oxo complexes **5** and **6**.^{7a,b} Such a sensitivity to water was already observed for [cp₂Ti(CO)₂].^{3,8} Complexes **3**, **4**, and **6** have been characterized by ¹H NMR spectra.⁹ With the X-ray diffraction studies reported in this work, structural information is available on all three representative members of the titanium(III)–titanium(IV) [L₆Ti₆O_{8–n}Cl_n] series. Pictures of complexes **2**¹⁰ and **3**¹¹ are shown in Figures 1 and 2, respectively. All these compounds have an octahedral metallic skeleton of six titanium atoms arranged centrosymmetrically. The faces of the octahedron are capped by triply bridging oxygen and chlorine atoms. Coordination geometry around Ti is a square pyramid having the basal plane defined by the heteroatoms Cl, O, and the apex by cyclopentadienyl ligands. Displacements from the basal plane of titanium are, for Ti1, Ti2 in complex **2**, 1.021 (2) and 1.025 (2) Å and, for Ti, Ti2, and Ti3 in complex **3**, 0.963 (3), 0.972 (3), and 0.947 (3) Å, respectively. While in the two regular octahedron clusters L₆Ti₆O₈ the Ti–Ti and Ti–O distances remain similar (averaging to 2.891 and 1.973 Å, respectively),^{8b} these separations are highly affected by the substitution of oxygen by chlorine (see caption of figures); complexes **2** and **3** have significantly elongated octahedral shape. The Ti–O and Ti–Cl bond distances are in agreement with the existence of a single bond.

A significant aspect of this chemistry is the electronic configuration of such organometallic aggregates.^{12,13} Complexes **1** and

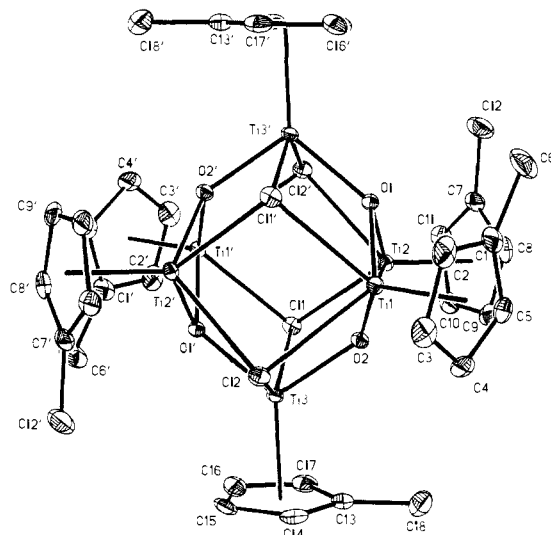


Figure 1. ORTEP view of [(η⁵-C₅H₄CH₃)Ti]₆O₄Cl₄ (**2**) (30% probability ellipsoids). Selected bond distances (Å): Ti1–O1, 1.972 (4); Ti1–O2, 1.962 (4); Ti1–Cl1', 2.623 (2); Ti–Cl2, 2.684 (2); Ti1–Cm1, 2.046 (7); intertitanium distances range from 2.838 (2) to 3.450 (2) Å. Bond angles at chlorines range from 81.9 (1)° to 85.5 (1)°; bond angles at the oxygens vary from 92.2 (2)° to 122.9 (2)°. Cm1 refers to the centroid of the ring Cl⋯C5 (Cm ≡ cp'). Prime indicates a transformation of $\bar{x}, 1 - y, \bar{z}$.

(5) [(η⁵-MeC₅H₄)TiCl(μ-O)]₄ was prepared by a variation of the method published by: Petersen, J. L. *Inorg. Chem.* **1980**, *19*, 181–185.

(6) Complex **2**: Aluminum powder (0.24 g, 8.75 mmol) and a catalytic amount of HgCl₂ were added to the solution of [cpTiCl(μ-O)]₄ (1.38 g, 1.94 mmol) in THF (50 mL). Stirring overnight resulted in a dark green mixture from which unreacted aluminum was filtered out. Diethyl ether was then added to the filtrate. Subsequent cooling at 2 °C for 14 days afforded dark grey plates of cp'₂Ti₆O₄Cl₄ (0.23 g, 19%). Complex **2** has a magnetic moment of 2.89 μ_B at 290 K. Complex **3**: In a typical heterogeneous synthesis, [cpTiCl(μ-O)]₄ (1.64 g, 2.49 mmol) in THF (60 mL) was stirred with zinc dust (0.62 g, 9.52 mmol) and HgCl₂ (catalytic amount) for 12 h resulting in a royal blue mixture which was filtered hot to remove unreacted zinc. Concentration and subsequent cooling afforded deep blue crystals of the dichlorinated compound cp₂Ti₆O₆Cl₂ (possibly as THF adduct, yield 0.46 g, 30%). Similar reductions with magnesium powder (molar proportion Ti:Mg = 4:1), sodium sand (Ti:Na = 2:1), and lithium nitride (Ti:Li₃N = 4:1) or of [(cpTiCl₂)₂(μ-O)] with zinc dust (excess zinc) gave same yields. The compound was also prepared homogeneously by reduction of [(cpTiCl₂)₂(μ-O)] (0.50 g, 1.30 mmol) in toluene (50 mL) by using (*n*-C₄H₉)₃SnH (0.8 mL, 2.9 mmol) at 25 °C. From the resulting dark blue-green mixture, crystals of cp₂Ti₆O₆Cl₂·2C₇H₈ (0.21 g, 24%) were obtained. Reduction of [cpTiCl(μ-O)]₄ with either tin hydride (Ti:H⁻ = 1:1) in toluene at 82 °C or LS-selectride (Ti:H⁻ = 2:1) in THF gave the same results.

(7) (a) The progressive hydrolyses of compounds **3** and **4** (solutions in pyridine-*d*₅) to the oxo aggregates **5** and **6**, respectively, were followed by NMR spectroscopy in sealed probes containing trace amounts of H₂O. The oxo derivatives can be prepared by refluxing a mixture of the dichloro compound and a few drops of degassed H₂O in toluene, from which copper-colored crystals of the product precipitate after several hours. (b) The X-ray structure determination of **5** is reported in ref 3; that of **6** is our unpublished result.

(8) Bottomley, F.; Egharevba, G. O.; White, P. S. *J. Am. Chem. Soc.* **1985**, *107*, 4353–4354.

(9) **3**: ¹H NMR (C₅D₅N, 300 MHz) δ 6.69 (br s). **4**: ¹H NMR (C₅D₅N, 300 MHz) δ 6.54 (br m) and 6.20 (br m) (η⁵-C₅H₄CH₃), 2.58 (br s) (η⁵-C₅H₄CH₃). **6**: ¹H NMR (C₅D₅N, 300 MHz) δ 6.17 (m) and 6.01 (m) (η⁵-C₅H₄CH₃), 2.39 (s) (η⁵-C₅H₄CH₃).

(10) Crystal data for complex **2**: C₃₆H₄₂Cl₄O₄Ti₆, *M*_r = 967.9, triclinic, space group *P* $\bar{1}$, *a* = 11.486 (7) Å, *b* = 10.150 (7) Å, *c* = 9.581 (6) Å; α = 98.79 (3)°, β = 108.96 (3)°, γ = 108.21 (3)°; *V* = 962 (1) Å³, *Z* = 1; *D*_c = 1.670 g cm⁻³; λ(Mo Kα) = 0.7107 Å, μ(Mo Kα) = 13.2 cm⁻¹; crystal dimensions 0.37 × 0.40 × 0.55 mm. Intensities of 3777 reflections were measured at room temperature (3 < θ < 26°) on a Philips PW 1100 diffractometer using Mo Kα radiation. The structure was solved by the heavy-atom method and refined anisotropically by full-matrix least squares, the number of parameters refined being 226. All calculations were carried out by using the SHELX-76 program. For 2507 unique observed reflections [*I* > 3σ(*I*)], the final *R* value was 0.039 (*R*_w = 0.040).

(11) Crystal data for complex **3**: C₃₀H₃₀Cl₂O₆Ti₆·2C₇H₈, *M*_r = 1029.2, monoclinic, space group *P*2₁/*c*, *a* = 13.190 (3) Å, *b* = 12.156 (2) Å, *c* = 14.665 (4) Å; β = 109.24 (2)°; *V* = 2220 (9) Å³, *Z* = 2; *D*_c = 1.540 g cm⁻³; λ(Mo Kα) = 0.7107 Å, μ(Mo Kα) = 13.2 cm⁻¹; crystal dimensions 0.20 × 0.47 × 0.72 mm. Intensities of 3400 reflections were measured at room temperature (3° < θ < 23°) on a Philips PW 1100 diffractometer using Mo Kα radiation. Solution and calculations for **3** were as for **2**, the number of parameters refined being 232. For 1452 unique observed reflections [*I* > 3σ(*I*)] the final *R* value was 0.067 (*R*_w = 0.069).

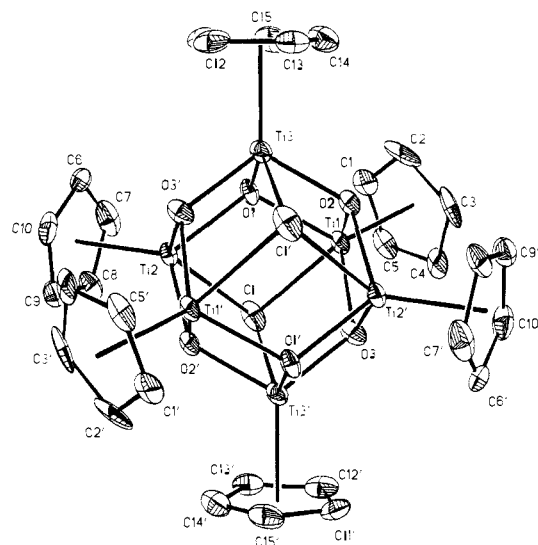


Figure 2. ORTEP view of [(η⁵-C₅H₅)Ti]₆O₆Cl₂ (**3**) (30% probability ellipsoids). Selected bond distances (Å): Ti1–O1, 2.006 (8); Ti1–O2, 2.088 (8); Ti1–O3, 2.005 (9); Ti1–Cl, 2.567 (5); Ti1–cp1, 2.04 (1); intertitanium distances range from 2.926 (4) to 3.335 (4) Å. Bond angles at chlorines range from 73.7 (1)° to 79.0 (1)°; bond angles at the oxygens vary from 96.4 (1)° to 129.3 (4)°. cp1 refers to the centroid of the ring Cl⋯C5. Prime indicates a transformation of $1 - x, \bar{y}, \bar{z}$.

2 contain two unpaired electrons, while complexes **3** and **4** are diamagnetic. The number of electrons in excess to those required for Ti–L, Ti–O, and Ti–Cl bonding increases precisely with the formal number of Ti(III) d¹ ions present in each aggregate: six in **1** and **2**, four in **3** and **4**, and two in **5** and **6**. While MO calculations explain the diamagnetism of **5** and **6** by placing the two excess electrons in the lowest a_{1g} orbital of the suggested scheme,¹³ a modified scheme, taking into account the lower symmetry when two or four oxygen atoms are replaced by chlorine, is needed for explaining the magnetic properties of **1–4**, having four and six electrons in excess to required for inert gas formalism.

(12) Trinh-Toan; Teo, B. K.; Ferguson, J. A.; Meyer, T. J.; Dahl, L. F. *J. Am. Chem. Soc.* **1977**, *99*, 408–416.

(13) Bottomley, F.; Grein, F. *Inorg. Chem.* **1982**, *21*, 4170–4178 and references therein.

The synthetic methodology reported, consisting of the use of specific reducing agents on oxochloro complexes, seems to be a good route for the preparation of electron-rich and functionalizable organometallic oxo aggregates.

Acknowledgment. We thank the National Science Foundation (Columbia University Grant CHE-8512660) and Italian C.N.R. (University of Parma) for financial support.

Supplementary Material Available: Crystallographic data (Table I), fractional atomic coordinates (Tables II, III), thermal parameters (Tables IV, V), and bond distances and angles (Tables VI, VII) for complexes 2 and 3 (6 pages). Ordering information is given on any current masthead page.

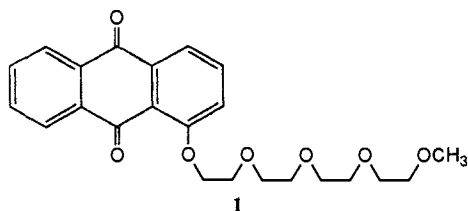
Enhanced Transport of Li^+ through an Organic Model Membrane by an Electrochemically Reduced Anthraquinone Podand

Lourdes Echeverria, Milagros Delgado, Vincent J. Gatto, George W. Gokel, and Luis Echegoyen*

Department of Chemistry, University of Miami
Coral Gables, Florida 33124

Received July 21, 1986

The neutral ligand **1** is unable to transport Li^+ to an appreciable



extent across a CH_2Cl_2 model membrane system. After electrochemical reduction to the corresponding anion radical $\mathbf{1}^{\cdot-}$, a Li^+ transport rate of 2.2×10^{-7} mol/h was measured. This constitutes a new method to effect enhanced binding and transport via an electrochemical "switching" mechanism for cations in solution. Direct ESR spectral evidence is presented which shows unequivocally the existence of a strong ion pair between the electrochemically generated $\mathbf{1}^{\cdot-}$ and Li^+ in the CH_2Cl_2 model membrane phase.

The idea of binding and transport enhancement of cations by ligands via an external switching mechanism has received considerable attention in recent years.¹ Most notable is the work of Shinkai et al. who have used light-induced isomerization of azo linkages to obtain binding and transport enhancement of metal cations.^{1a,b} Izatt and co-workers were able to enhance transport rates via pH gradients using calixarene and pyridone carriers, a process triggered by deprotonation of the ligand in the cation source interphase and reprotonation in the receiving phase.^{1c,d} An intermediate anionic carrier species and a neutral cation-ligand complex are involved in this process, a similar situation to that presented in this work. Another recent paper related to this work reported enhanced Na^+ transport rates across liquid membranes via an electrochemical "pumping" process.^{1e} Our approach to switching and binding enhancement of alkali-metal cations involves electrochemical reduction of ligands which yield relatively stable anion radicals.² Nitrobenzene-^{2a} and anthraquinone-^{2b} substituted

(1) (a) Shinkai, S.; Shigematsu, K.; Kusano, Y.; Manabe, O. *J. Chem. Soc., Perkin Trans. 1* **1981**, 3279. (b) Shinkai, S.; Inuzuka, K.; Miyazaki, O.; Manabe, O. *J. Am. Chem. Soc.* **1985**, *107*, 3950. (c) Izatt, R. M.; Lamb, J. D.; Hawkins, R. T.; Brown, P. R.; Izatt, S. R.; Christensen, J. J. *J. Am. Chem. Soc.* **1983**, *105*, 1782. (d) Izatt, R. M.; Lindh, G. C.; Clark, G. A.; Bradshaw, J. S.; Nakatsuji, Y.; Lamb, J. D.; Christensen, J. J. *J. Chem. Soc., Chem. Commun.* **1985**, 1676. (e) Saji, T. *J. Chem. Soc., Chem. Commun.* **1986**, 716.

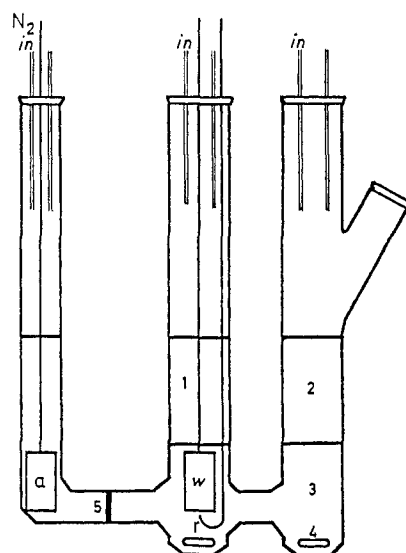


Figure 1. Diagram of transport cell: (1) source phase (1 M LiClO_4 in H_2O); (2) receiving phase (deionized water); (3) membrane phase (2 mM **1** and 0.1 M TBAP in CH_2Cl_2); (4) magnetic bar; (5) fine porosity glass filter; (a) Pt auxiliary electrode; (w) Pt working electrode; (r) Ag wire reference electrode.

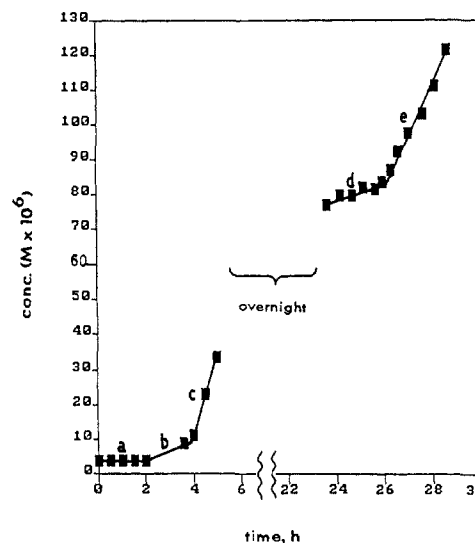


Figure 2. Plot of the Li^+ concentration in the receiving phase as a function of time: (a) transport by neutral **1**; (b) and (d) transport during the reduction of **1** to $\mathbf{1}^{\cdot-}$; (c) and (e) transport by $\mathbf{1}^{\cdot-}$. Note the discontinuity in the time axis during the overnight period. Some transport took place during that time since some $\mathbf{1}^{\cdot-}$ was still present.

lariat ethers and podands have been extensively investigated by using cyclic voltammetry. Cation binding enhancement factors as high as 10^6 for Li^+ have been reported.^{2a}

Figure 1 shows a diagram of the transport cell used. The model membrane, **3** in Figure 1, consisted of a 0.1 M tetra-*n*-butylammonium perchlorate solution containing 2 mM **1** in CH_2Cl_2 . The donor water phase, **1** in Figure 1, contained 1 M LiClO_4 and the receiving water phase, **2** in Figure 1, was deionized water. Transport of Li^+ was monitored by measuring the Li^+ concentration in the receiving phase at 20–30-min intervals using atomic absorption spectrophotometry (Perkin-Elmer Model 403). Two magnetic bars, **4** in Figure 1, were used to ensure effective mixing during the course of the experiment.

(2) (a) Kaifer, A.; Gustowski, D. A.; Echegoyen, L.; Gatto, V. J.; Schultz, R. A.; Cleary, T. P.; Morgan, C. R.; Goli, D. M.; Rios, A. M.; Gokel, G. W. *J. Am. Chem. Soc.* **1985**, *107*, 1958. (b) Echegoyen, L.; Gustowski, D. A.; Gatto, V. J.; Gokel, G. W.; *J. Chem. Soc., Chem. Commun.* **1986**, 220. (c) Gustowski, D. A.; Delgado, M.; Gatto, V. J.; Echegoyen, L.; Gokel, G. W. *Tetrahedron Lett.* **1986**, 3487.